Advancing Direct Air Capture via Wood-Derived Biochar: Catalytic Enhancement of CO_2 Adsorption Performance and Regeneration Stability

A THESIS
SUBMITTED TO THE FACULTY OF THE GRADUATE SCHOOL
OF THE UNIVERSITY OF MINNESOTA
BY

Jannatul Adnin Eshita

IN PARTIAL FULFILLMENT OF THE REQUIREMENTS
FOR THE DEGREE OF
MASTER OF SCIENCE

Chair: Dr. Sam Toan
Co-Chair: Dr. Maohong Fan

June, 2025

Acknowledgements

I would like to extend my heartfelt gratitude to my advisor, Dr. Sam Toan, as well as my co-supervisors, Dr. Maohong Fan and Dr. Remanul Islam. Their guidance, patience, and expertise were essential throughout all phases of this research. Their mentorship not only directed the technical aspects of this work but also had a significant impact on my development as a researcher. I am truly grateful to my labmate, Hafsa Habib; lab coordinator, Lyndon Ramrattan; and Sean Xiang Tang from the University of Wyoming for their unwavering support. Special thanks go to the faculty and staff of the Department of Chemical Engineering at the University of Minnesota Duluth. The academic support they provided, along with the collaborative atmosphere they nurtured, equipped me with the tools and opportunities needed to complete this work. Lastly, I am deeply grateful to my friends and family for their unwavering encouragement and understanding. Their belief in me was a continuous source of motivation throughout the challenges encountered during this research journey.

Dedication

To my husband, Samiul Mushfik, and my friend, Hafsa Habib, for their unwavering support

Abstract

Wood-derived biochar offers a sustainable and cost-effective method for direct air capture (DAC) of CO_2. This study comprehensively examines the impact of operating temperature, gas flow rate, and prolonged saturation on CO_2 adsorption performance. A biochar-packed fixed bed column was subjected to synthetic air (400 ppm CO_2 and balanced N_2) at various flow rates (35–80 mL/min) and temperatures (5°C to 20°C). The biochar exhibits a highly alkaline nature (pH 10.23), high specific surface area, and a rich microporous structure. Maximum CO_2 removal occurred at lower temperatures and flow rates, resulting in a CO_2 removal rate of up to 91.8% and an adsorption capacity of 0.014 mmol/g at 5°C. Although higher flow rates enhanced adsorption capacity, they reduced removal efficiency. After 12 hours of continuous exposure, saturation behavior was observed, resulting in a total adsorption capacity of nearly 0.055 mmol/g (2.42 mg/g). Kinetic analysis revealed good agreement with both pseudo-second-order (PSO) and pseudo-first-order (PFO) models, indicating the coexistence of physisorption and chemisorption mechanisms. The adsorbent consistently demonstrated stable performance across several regeneration cycles, highlighting its reusability. These results highlight the promise of wood biochar as a viable, renewable DAC sorbent capable of capturing low-concentration CO_2 across different environmental conditions.

Contents

List of Tables

List of Figures

Chapter 1

Introduction

Climate change is one of the most significant challenges facing the planet at present. Rapid industrialization and population growth have significantly increased CO_2 emissions, accelerating global warming and disrupting ecosystems through drought, flooding, and glacial melt [1]. According to NASA and NOAA, due to industrialization that began in the 18th century, atmospheric CO_2 increased rapidly by 50% compared to 1850. CO_2 rose from 365 ppm in 2002 to over 428 ppm in March 2025, an approximately 17% increase over the last 23 years. CO_2 is the most significant radiative forcing greenhouse gas that does not condense and has the longest lifespan in the atmosphere. It can remain in the atmosphere for thousands of years [2]. A significant reduction in carbon dioxide emissions is essential; otherwise, constraining global warming to 1.5 °C or even 2 °C will be unreachable [3]. Scientists and engineers are developing various carbon capture and removal technologies to decrease the atmospheric carbon dioxide (CO_2) concentration and mitigate global warming [2].

Direct air capture (DAC) is a promising solution among all existing carbon dioxide removal technologies. It can capture CO_2 from any emission source and is flexible enough to be deployed in areas with low-cost or renewable energy availability [2]. In DAC, ambient air passes over a sorbent that selectively captures CO_2 and is released as a concentrated stream for further use [3]. A key challenge is the deterioration of sorbents due to reduced chemical stability and sorption performance after thousands of cycles in large amounts of air [4]. Another common challenge sorbents encounter is low carbon dioxide (CO_2) uptake at atmospheric concentrations (approximately 400

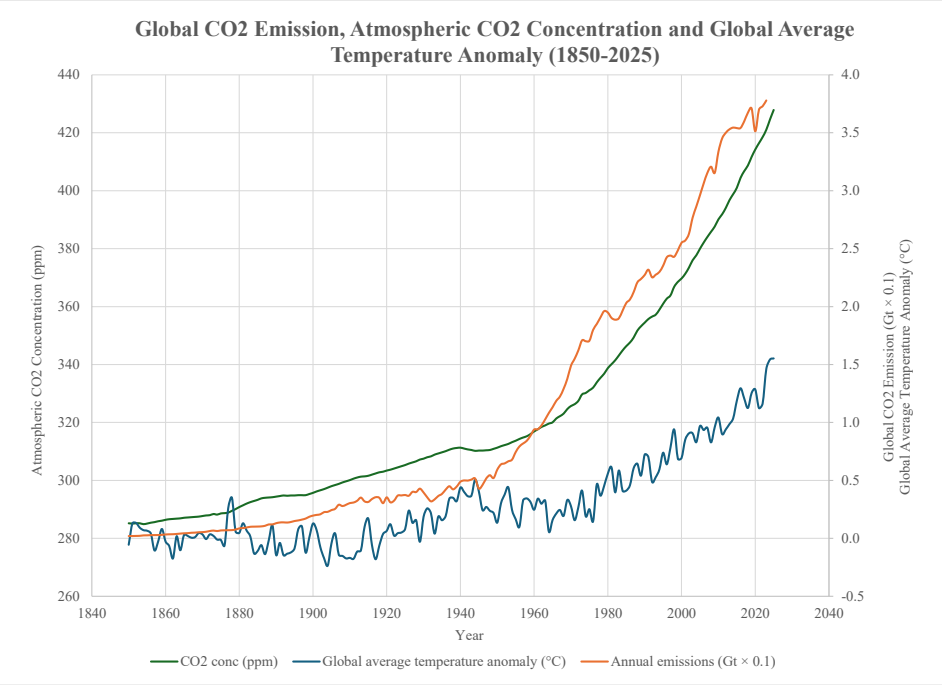

Figure 1.1: Long-term trends in global CO_2 emissions, atmospheric CO_2 concentration, and global mean temperature anomaly (1850–2025). The figure illustrates temporal variations in atmospheric CO_2 concentration (ppm), global annual anthropogenic CO_2 emissions (Gt $\times$ 10^1), and global average surface temperature anomaly (°C). These trends highlight the strong correlation between anthropogenic CO_2 emissions and the concurrent rise in atmospheric CO_2 levels and global temperatures. Data sources: NASA GISS (data.giss.nasa.gov), NOAA (gml.noaa.gov), and Our World in Data (ourworldindata.org).

ppm), restricted long-term stability, and higher energy requirements for the regeneration process. Therefore, developing robust, cost-effective adsorbents with high adsorption capacity and low energy consumption is essential to enable practical and scalable DAC applications [5].

Direct air capture (DAC) requires materials that can efficiently and affordably remove carbon dioxide, mainly in outdoor air conditions [5]. Amine solution as a liquid phase sorbent currently dominates the CO_2 capture industry. Nevertheless, it imposes a considerable energy cost and can corrode equipment. In contrast, solid sorbents provide advantages like lower capital expenses, enhanced efficiency, and less waste generation compared to amine-based sorbents [6]. Solid sorbents can capture CO_2 through physisorption or chemisorption. Sorbents like CaO and $Ca(OH)_2$ exhibit higher adsorption rates for inorganic chemisorption but only above 400 °C [7]. $NaHCO_3$, Na_2CO_3, and NaOH have shown low adsorption rates and high regeneration temperatures of over 927 °C [8]. On the other hand, solid absorbents, which depend mainly on physical adsorption, provide a more energy-efficient alternative to chemical adsorption [9]. Materials like activated carbon, zeolites, and MOFs have high surface areas and good CO_2 uptake capacities. However, their high cost and strong CO_2 binding make regeneration challenging and potentially expensive for large-scale use [10, 11]. Solid sorbents such as activated carbon (AC) and biochar provide physically driven adsorption mechanisms that are more energy efficient and potentially easier to regenerate. The extremely high surface area of AC boosts its adsorption capabilities under high pressures; however, it reduces capture capacities at low pressures and leads to weak selectivity for CO_2 and N_2, making it less ideal for DAC [3]. Furthermore, surface modifications (including amine or metal oxide functionalization) increase both cost and complexity, despite their ability to enhance CO_2 adsorption [10]. AC is costly due to the high pyrolysis temperatures (up to 950 °C) and chemical activating agents (e.g., $ZnCl_2$ or KOH) needed. These production methods create economic and environmental challenges, especially when considering large-scale deployment [10]. In contrast to AC, biochar can be created from inexpensive agricultural and forestry byproducts using a straightforward slow pyrolysis process at moderate temperatures (300–600 °C). This approach eliminates the need for energy-intensive activation processes or chemical treatments, making it at least ten times more cost-effective and environmentally sustainable [12].

Moreover, its porous structure, coupled with a high surface area-to-weight ratio and polar, frequently hydrophilic surfaces, positions it as a strong contender for physical CO_2 adsorption. Even if biochar shows lower uptake than chemically active sorbents, its low cost and potential for soil amendment allow for dual-purpose use without the need for complex regeneration [10]. Wood-derived biochar is recognized for its high carbon content and significant activation potential modification [6]. Due to several key advantages, biochar shows great potential for future carbon capture applications. These include the availability of inexpensive feedstock from various biomass waste for biochar production, the ability to repurpose used biochar, its superior adsorption characteristics compared to other organic chemicals like MOFs in bulk gas adsorption, its cost-effectiveness, environmental sustainability, and the option for easy customization [6]. While earlier research has investigated biochar for capturing CO_2 from post-combustion flue gas, there has been insufficient focus on its effectiveness in real direct air capture (DAC) scenarios, especially in dry air situations. Factors influencing biochar performance in DAC require further exploration for the process development [13]. Addressing this knowledge gap is essential for assessing biochar's practical application in scalable DAC systems under ambient conditions [10, 3].

This study intends to assess the feasibility of wood-derived biochar as an economical and sustainable sorbent for CO_2 capture in DAC scenarios. It specifically seeks to examine how temperature and flow rate influence adsorption performance, evaluate kinetic behavior with PFO and PSO models, and investigate the reusability of biochar through cyclic adsorption experiments.

Chapter 2

Experiment Methodology

METHODS AND MATERIALS

Materials Preparation

The wood biochar used in this study was sourced from Plantonix. A 10 g sample was weighed and degassed at 120°C for 20 hours under a nitrogen (N_2) flow rate of 100mL/min to remove moisture and residual gases[14]. The degassed sample was cooled to 25°C while maintaining the same N_2 flow [15].

pH Test

The pH of biochar was determined by suspending 1 g of biochar in 10mL of deionized water (1:10 ratio) and equilibrating the mixture for 1 hour. The pH meter was calibrated with buffer solutions at pH 4, 7, and 10, and the measurement was made by inserting a glass H^+ electrode into the supernatant [16].

BET Surface Area Analysis

BET and Langmuir surface area measurements were performed using Quadrasorb evo / Quantachrome at 77K. Samples were degassed at 110°C for 8 hours using FLOVAC Degasser prior to N_2 physisorption experiments.

Selectivity Test

TGA analysis was conducted to understand the selectivity of CO_2 over other gases, prominently present in the dry air (N_2 and O_2). Four comparative cyclic test runs were conducted using four different gas compositions:(20% O_2, 80% N_2), (300 ppm CO_2, 20% O_2, 80% N_2), 100% N_2, and (1% CO_2, 99% N_2). The mass and temperature change datasets were plotted against time over these four cycles. A 13.5 mg biochar sample was placed in a TGA pan and dried at 110°C for 240 min under a 10 mL/min nitrogen purge to remove moisture and pre-adsorbed gases corresponding to the weight loss during this segment. Following degassing, the system was cooled to ambient temperature while switching to the test gas, which was used during both the ramp-down and subsequent 240-minute isothermal adsorption phase. The TGA continuously monitored mass changes throughout. The net mass gain (Δm) was calculated as the difference between post-drying and adsorption mass.

CO_2 Capture Experiment

The CO_2 adsorption capacity of the wood biochar was evaluated using volumetric analysis with a CAI ZPA Non-Dispersive Infrared (NDIR) Gas Analyzer. The Gas Analyzer measures CO_2 concentration in ppm up to 1000 ppm in the gas stream. Monarch Data Logger records and stores data for further analysis, including CO_2 concentration and temperature. For each experiment, 2g of degassed biochar was weighed and packed into a vertical glass tube to make the adsorption column. Two gas mixtures, 100% nitrogen and air (400 ppm CO_2 + balanced N_2), were purchased from Linde and used for each. The gas tanks have their regulators set to 100 psi. The gas flow was regulated using Red-y Smart Series Mass Flow Controllers (MFCs) controlled by the Red-y software on a laptop. A thermocouple, inserted into the column and connected to a Monarch Data Logger, recorded the temperature. A Thermo Neslab Digital Plus RTE-17 chiller regulated the water bath temperature, enabling adsorption and desorption tests at controlled temperatures.

Adsorption

Adsorption experiments were conducted at varying temperatures (from 0°C to 20°C) and 1 atm pressure. The chiller was turned on to cool the water bath to the required temperature. Ready software was opened to set the flow rate for two MFCs. Before

every experimental run, the gas analyzer was calibrated, and the test lines were purged. The nitrogen valve (N_2) valve was opened for zero calibration, and the flow was set at 200 ml/min. Once the gas analyzer reading stabilized, it was calibrated to zero for the baseline readings of 0 ppm CO_2 in channel 1. Once the zero calibration was completed, the N_2 flow was set to zero, and the valve was closed. Then, air was introduced at the same rate for the span calibration of the analyzer at 400 ppm CO_2. Finally, the system, including the adsorption column, was purged again with N_2 to return the baseline to 0 ppm.

The vertical adsorption column was sealed with a rubber stopper fitted with inlet and outlet gas tubes and a temperature sensor. The column was immersed in the temperature-controlled water bath to reach the target temperature. Air was introduced into the packed column at varying lower flow rates through the MFC. A supplementary N_2 flow was added before the gas analyzer, ensuring the required total flow of 200 mL/min. The gas analyzer measures the concentration of unabsorbed CO_2 in the effluent gas for 1 hour. After adsorption, all gas flows were stopped, and the data were retrieved from the Data Logger and exported to Rcloud for analysis. After that, the system was ready for the desorption test.

Desorption

Desorption was performed by heating the column to 70°C and purging with N_2 at 200 ml/min for 60 minutes to remove weakly adsorbed gases. The column was submerged in a heated water bath maintained by a recirculating system. A thermocouple recorded temperature inside the column.

The gas analyzer was calibrated, and the system, except the adsorption column, was purged for desorption. The N_2 valve is opened completely to purge the flow lines connected to the gas analyzer of CO_2. After calibration, N_2 passed through the biochar packing column at 200 ml/min for 1 hour. CO_2 was desorbed from the wood biochar, and the gas analyzer measured the CO_2 concentration in the effluent gas. After desorption, the N_2 flow was stopped, and the data were retrieved from the Data Logger and exported to Rcloud for analysis.

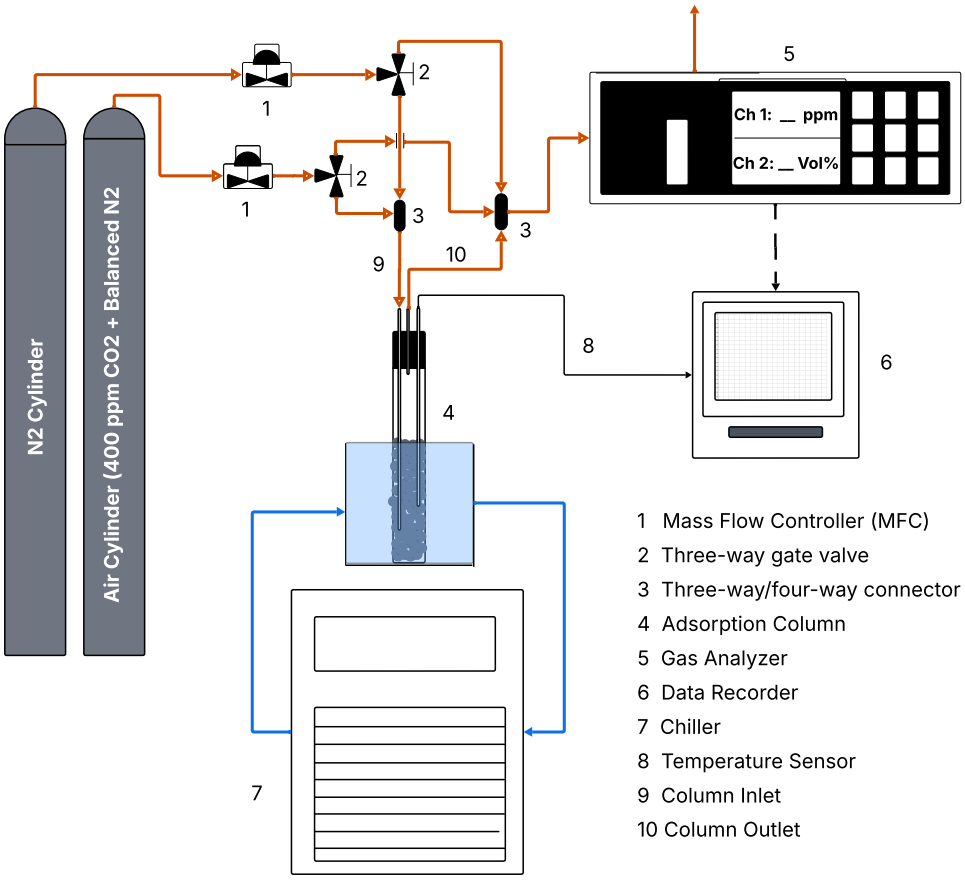

Figure 2.1: Schematic of the fixed-bed experimental setup for CO_2 capture under direct air capture (DAC) conditions. The system includes a mass flow controller (1) to regulate gas flow, a three-way gate valve (2) and connectors (3) for switching gas streams, and an adsorption column (4) packed with biochar. A gas analyzer (5) connected to a data recorder (6) monitors outlet CO_2 concentration. Temperature is controlled using a chiller (7) and measured by a sensor (8). Air or N_2/CO_2 mixtures enter at the column inlet (9) and exit at the outlet (10).

Adsorbent Regeneration and Reusability

To evaluate the reusability and long-term stability of the wood biochar, 10 consecutive adsorption-desorption cycles were conducted. A new 2g sample was degassed and weighed, packed into the column for the cycle tests. For the adsorption, 35 ml/min of air was used for 1 hour at ambient temperature. After completing the initial adsorption stage, the adsorbent was regenerated by heating the column to 70°C and maintaining this temperature for 1 hour under a continuous nitrogen (N_2) flow of 200 ml/min. Following regeneration, the column was allowed to cool down to ambient temperature. The adsorption procedure was then repeated under the same experimental conditions. After each cycle, data were retrieved from the Data Logger and analyzed to monitor the CO_2 uptake performance and assess any loss in adsorption capacity across cycles.

Adsorption Kinetics

Adsorption modeling requires kinetic and diffusion models to understand the rate-controlling steps and mass transfer mechanisms [17]. Kinetic models help describe fast adsorption and analyse mass transfer limitations and residence time, adsorption isotherms characterize equilibrium behaviour, and design and optimize sorbent performance [17]. Although research interest in DAC has increased, how sorbent characteristics influence CO_2 adsorption under DAC conditions remains poorly understood from a modelling standpoint [42]. Recent work (e.g., Liu et al.) has highlighted the need for simplified yet effective kinetic models for DAC. While some detailed models are suitable for process-level optimization, bench-scale experimentalists who need practical tools to fit breakthrough curves face a gap. Liu et al.'s model provides a minimal kinetic framework that bridges this gap and allows researchers to explore how flow rate, humidity, and temperature affect adsorption [42]. In this study, kinetic behaviour will be measured using PFO and PSO models.

Pseudo-First Order (PFO) Model

Pseudo-first order (PFO) is the simplest kinetic model that predicts the adsorption rate to the adsorption sites [17]. This model is often used to represent the liquid-solid phase [19]. It assumes the rate is proportional to the number of open sites:

$$\frac{dq_t}{dt} = k_1(q_e - q_t) \tag{2.1}$$

Where k_1 is the rate constant of PFO adsorption, q_e is the amount of adsorbate concentration in the solid phase at equilibrium (mg/g), and q_t is the amount of adsorption at any given time t. Integration with boundary conditions $q_t = 0$ at $t = 0$ and $q_t = q_e$ at $t = t$ gives:

$$q_t = q_e(1 - e^{-k_1 t}) \tag{2.2}$$

A simplified linear form:

$$\ln(q_e - q_t) = \ln q_e - k_1 t \tag{2.3}$$

Pseudo-Second Order (PSO) Model

The pseudo-second-order (PSO) Model describes adsorption based on chemical interactions. It predicts the adsorption rate as the square of the available adsorption sites [17]. Many researchers have used this model to explain the experimental data of CO_2 adsorption kinetics [20].

$$\frac{dq_t}{dt} = k_2(q_e - q_t)^2 \tag{2.4}$$

Where k_2 is the PSO rate constant, q_e is the amount of adsorbate concentration in the solid phase at equilibrium (mg/g), and q_t is the amount of adsorption at any given time t. Integration with boundary conditions $q_t = 0$ at $t = 0$ and $q_t = q_e$ at $t = t$ gives:

$$q_t = \frac{q_e^2 k_2 t}{1 + q_e k_2 t} \tag{2.5}$$

Linearized form:

$$\frac{t}{q_t} = \frac{1}{q_e^2 k_2} + \frac{t}{q_e} \tag{2.6}$$

The initial adsorption rate is:

$$h = k_2 q_e^2 \tag{2.7}$$

Activation energy can be determined using the Arrhenius equation:

$$k = k_0 e^{-E_a/RT} \tag{2.8}$$

k_0, E_a, R and T are the initial rate constant, the apparent activation energy for adsorption, the gas constant, and the adsorption temperature in K, respectively.

Besides delivering the adsorption rate constant for CO_2 adsorption, the PSO model helps determine the adsorption capacity under equilibrium conditions. The PSO model proposes that the rate-limiting step is driven by chemical bonding, particularly covalent interactions, between the adsorbate and the surface of the sorbent [17, 21].

The adsorption kinetics of CO_2 capture on activated carbon surfaces have been studied using the PFO and PSO models under different pressure and temperature conditions. Several studies have reported the PSO model as a better fit than the PFO model [22]. For example, Sadaf and Bhatti found that the PSO model is an appropriate fit to describe the biosorption of Indosol orange RSN dye by peanut husk biomass [23]. Similarly, the study by Borhan and Suzana revealed that the CO_2 adsorption kinetics on rubber-seed shell-derived activated carbon best fit the PSO model (R2 = 0.9388) compared to the PFO model (R2 = 0.8392) [20]. The adsorption kinetics studies on CO_2 capture on lignocellulosic-based activated carbon done by Rashidi also revealed the conformity of the PSO model with the experimental data, where initial adsorption rate (h) values (decreasing with temperature) indicated the physisorption and exothermic behavior of this process [19].

Chapter 3

Results and Discussion

3.1 pH Test

The pH values of four biochar samples were measured to assess their alkalinity. The results are summarized in table 1.

Table 3.1: pH Characterization of Wood Biochar Samples in Deionized Water Suspension (1:10 w/v Ratio)

Sample	**pH value**
Sample 1	10.26
Sample 2	10.13
Sample 3	10.31
Sample 4	10.23
Average	10.23

All samples showed a strongly alkaline nature, with pH values between 10.13 and 10.31, averaging 10.23±0.07. The high pH of the biochar suggests the presence of basic mineral components like K, Ca, and Mg oxides [24], which are typically preserved during pyrolysis. These alkaline earth metals can enhance biochar's ability to adsorb acidic CO_2, resulting in a greater capacity for CO_2 adsorption. Thus, the mineral-derived basic sites on high-pH biochars act as active centers that strongly bind or react with CO_2, resulting in a higher adsorption capacity compared to neutral or low-pH carbons. Basic surface functional groups are essential for CO_2 adsorption in biochar, as they enhance its surface basicity and increase the biochar's affinity for CO_2. Biochar containing metal oxides and amine-functionalized groups can facilitate CO_2 capture and

form carbonates, bicarbonates, or minerals [25].

Xu et al found that adsorption occurred through both physical and chemical means. Physical sorption primarily depended on the surface area and pore volume, whereas chemical sorption was influenced mainly by the minerals present in biochar. He found that biochar with substantial Mg, Ca, and K content could uptake approximately 18-34 mg/g CO_2 at 25 °C, even without activation. A significant fraction of the capture happened due to chemical binding at basic sites, induced chemisorption via mineralogical reaction, accounting for roughly 18-51% of the total sorption [24]. Fidel et al. reported a high pH value of 10.3 for corn stover biochar with a substantial alkaline metal content of 63g/kg, further indicating the presence of rich basic substance and the likely contribution of chemisorption to the total CO_2 capture [16]. Xu also studied pig manure biochar, which showed an even higher alkaline metal content of approximately 98 g/kg and a pH of 10.4 [24]. In this case, chemisorption attributed to metal interactions accounted for 17.7% of the total CO_2 sorption.

Numerous studies have shown that enhancing the alkalinity of biochar improves its CO_2 capture performance. For example, KOH activation is commonly used to increase the basicity of biochar, thereby improving adsorption efficiency. Similar outcomes have been reported in studies involving activated carbon modified to target acidic pollutants, where increased surface basicity correlated with high removal rates [26]. The chemical principle underlying these interactions is broadly applicable. A study on direct air capture in seawater using biologically induced alkalinity demonstrated that an increase in alkalinity enhances CO_2 uptake by shifting the carbonate equilibrium towards bicarbonate and carbonate species [27].

3.2 BET Test

The wood-derived biochar showed a high BET specific surface area of approximately 572 m^2/g, a total pore volume of about 0.36 cm^3/g, and an average pore width of 1.36 nm. These values indicate a highly porous carbon structure. Sprue wood biochar produced via slow pyrolysis at 600°C had a BET surface area of approximately 465 m^2/g with a pore volume of 0.216 cm^3/g [28]. Mukherjee used coffee grounds to produce biochar, capturing CO_2 at 30–90 °C [29]. The maximum adsorption capacity of 2.8 mmol/g was achieved with a BET surface area of 539 m2/g biochar. Chemically activated biochar can achieve even higher surface properties. KOH-activated sunflower straw

biochar activated at 900°C showed the highest SSA, total pore volume and average pore size, 1032.361 m^2/g, 0.481 cm^3/g and 1.863 nm, where the sample activated at 600 °C exhibited SSA of 622 m^2/g, 0.272 cm^3/g and 1.748nm [30]. Compared to the literature data, the pore structures of the wood biochar sample in this study indicate highly porous structures. The relatively small average pore diameter (1.36 nm) further suggests that most of this surface are is due to micropores (pore width $<$ 2nm). CO_2 adsorption depends on mesopore volume for BET surface areas $<$ 500 m2/g and on micropore area for BET $> 500m2/g$ [31].

Table 3.2: Specific surface area, total pore volume, and average pore size of the wood-derived biochar sample

Sample	**BET Surface Area** S_{BET} (m^2/g)	**Langmuir Surface Area** S_L (m^2/g)	**Surface Area Ratio** = S_L / S_{BET}	**Total Pore Volume** V_{total} (cc/g)	**Micropore Volume** V_{micro} (cc/g)	**Pore Width** (nm)
Wood Biochar	572.2	774.4	1.35	0.3595	0.2147	1.36

The N_2 adsorption-desorption isotherm of the biochar indicated the presence of a hysteresis loop. This corresponds to a type profile according to the Brunauer, Deming, Deming, and Teller (BDDT) classification system [32]. This is characteristic of adsorption on porous solids via monolayer, multilayer adsorption, followed by capillary condensation taking place in pores. The isotherm also showed a hysteresis loop, which corresponds to the H3 or H4 type and the presence of narrow slit-like pores. The isotherm initially showed a steep adsorption up to p/p0 = 0.1, then the isotherm rather exhibits straight lines up to p/p0 =0.9. Finally, an upward trend near saturation pressure. At low partial pressure, the dramatic increase in volume indicates the presence of micropores. This structure aligns more with the monolayer adsorption model (Langmuir adsorption).

When the adsorption isotherm indicates the presence of a mesoporous carbon structure, the pore volume and average pore size indicate that the biochar is more microporous. Most adsorbents are heterogeneous porous media [43]. Micropores provide deep adsorption energy wells that can trap CO_2, so a large micropore volume directly

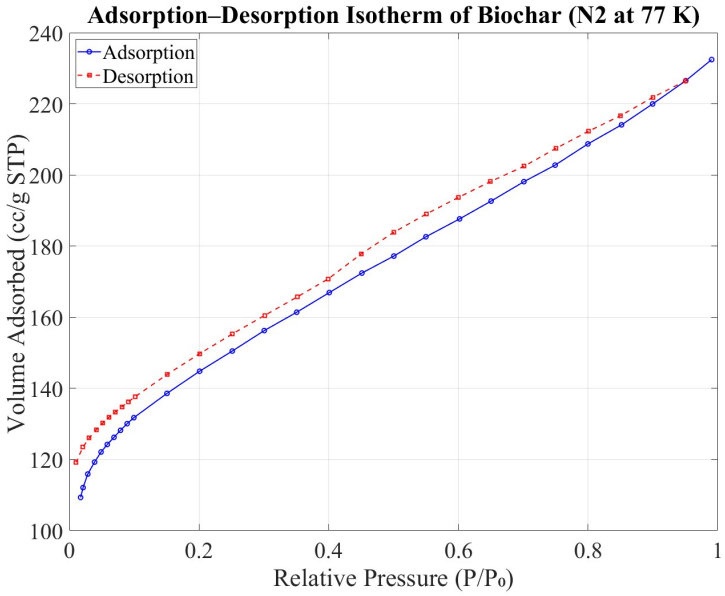

Figure 3.1: N adsorption–desorption isotherm of wood-derived biochar measured at 77K, indicating surface area and porosity characteristics.

translates to more adsorption sites and higher capacity. By contrast, larger mesopores (> 2 nm) contribute relatively little to CO_2 uptake at 1 atm, though they do improve diffusion pathways into the particle [31].

3.3 Selectivity Test

The thermo-gravimetric analysis (TGA) monitored the biochar's mass change (Δm) under different gas compositions at constant temperature. Four atmospheres were tested, revealing how the sample interacts with O_2, N_2, and trace CO_2. 100% N_2 exhibited the lowest weight change at 0.1395 mg. N_2 at ambient temperature has very low adsorptive capacity on carbon as it is non-polar and poorly condensable. The weight gain is most likely due to the N_2 filling at the microspores. 20% O_2/80% N_2 yielded a net mass gain (Δm) of 0.15388 mg, which is higher than N_2 alone. This relative increase in mass is attributed to O_2 uptake by the biochar, most likely via chemisorption on active surface sites. Carbon surfaces can bind O_2 even at modest temperatures, forming C-O complexes and increasing mass [34]. Biochar exhibited

a slight affinity for O_2, but this was primarily due to irreversible surface oxidation rather than reversible physical adsorption. O_2 is much less strongly held than CO_2 in carbon pores. The test with 300 ppm CO_2 in 20% O_2/80% N_2 showed the same mass gain as O_2/N_2 with no CO_2. The biochar did not add up any significant weight from 300 ppm CO_2, rather slight decrease in weight gain might indicate that CO_2 inhibited O_2 adsorption. CO_2 can occupy active sites or pore spaces, preventing O_2 from chemisorbing [35]. In low-rank coals, CO_2 has been reported to displace O_2 from pore walls physically [35].

The highest uptake (0.18483 mg) was observed with 1% CO_2 in 99% N_2, much higher than the other gas compositions. This unequivocally demonstrates the biochar's ability to adsorb CO_2 when its partial pressure is increased to 0.01 atm. TGA experiment with 1% CO_2 confirmed the a high intrinsic selectivity for CO_2 over N_2.

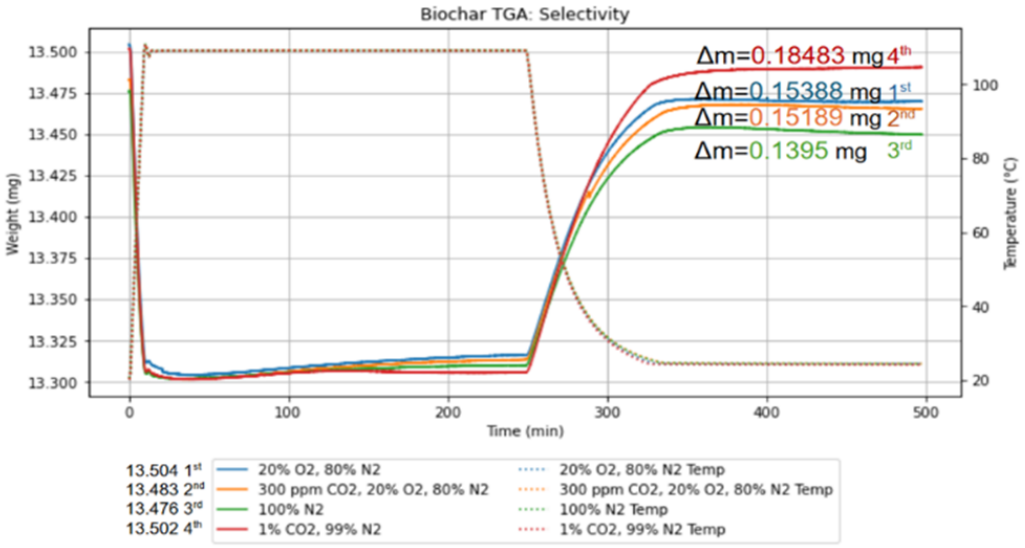

Figure 3.2: CO_2 selectivity of wood-derived biochar over N_2 and O_2, demonstrating preferential adsorption behavior under DAC-relevant conditions.

Pyrolyzed and activated biochars often show $\alpha(CO_2/N_2)$ around 4-10 under flue-gas conditions [36], and up to 12 for optimally activated samples [36]. The higher critical temperature and quadrupolar nature of CO_2 lead to greater adsorption forces in micropores, whereas N_2 and O_2 remain mostly in the gas phase [36]. Fewer studies

explicitly report CO_2/O_2 selectivity, but O_2 behaves similarly to N_2 as a weak adsorbate gas on carbon. Under a low partial pressure of CO_2 condition (300 ppm CO_2, 20% O_2 and 80% N_2), the biochar's uptake was essentially zero, which presents a serious challenge. The TGA result showed no significant adsorption, indicating negligible capture capacity at atmospheric CO_2 levels. Dan studied CO_2 with AC and revealed that carbons with many < 0.7 nm pores outperform other gases for low-pressure CO_2 capture [37]. The wood biochar's average 1.36 nm pore size is too large to develop the strong adsorption potential needed at 0.0004 atm partial pressure of CO_2. Therefore, pore-size optimization or surface functionalization is required to achieve meaningful DAC performance.

The wood biochar's high pH (10.23) indicates a surface rich in basic functional groups, which can promote CO_2 adsorption via acid-base interaction [6, 38]. This chemical basicity contributes to the material's preferential affinity for CO_2 over N_2 and O_2, as observed in the TGA experiments, where 1% CO_2 induced a significantly higher mass gain than either N_2 or O_2 environments. Such behavior is consistent with studies reporting that biochars with higher pH and basic surface sites exhibit greater CO_2/N_2 selectivity due to stronger interactions with the acidic CO_2 molecule [39]. For instance, nitrogen-doped or alkali-modified biochars with pH > 9 have demonstrated selectivity factors exceeding 10 under sub-atmospheric conditions [40, 41]. However, the lack of measurable CO_2 uptake at 300 ppm, despite the biochar's high surface area (572.2 m^2/g) and micropore volume (0.2147 cm^3/g), suggests that surface basicity alone is insufficient for DAC-level capture. Ultramicropores ($< 0.7nm$) are critical for adsorbing CO_2 at low partial pressures due to the need for overlapping adsorption potentials [42, 43]. The wood biochar's average pore width of 1.36 nm exceeds this optimal range, likely allowing CO_2 to diffuse without strong confinement. Therefore, while the alkaline pH supports inherent selectivity, effective DAC performance requires synergistic tuning of both surface chemistry and pore architecture [6, 39].

3.4 Effect of Inlet Air Flow Rate on CO_2 Adsorption Performance

The influence of inlet air flow rate on the CO_2 capture performance of wood biochar was investigated at ambient temperature (20 °C) and atmospheric pressure across four

different flow rates: 35, 50, 65, and 80 ml/min. As shown in Figure 3.3, the results indicate a clear trade-off between adsorption efficiency and adsorption capacity with increasing flow rate.

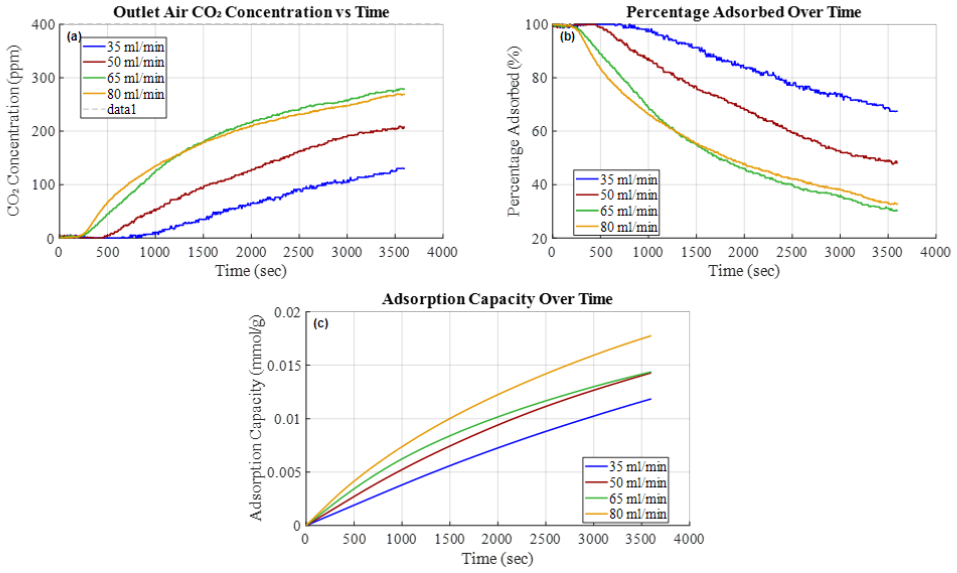

Figure 3.3: CO_2 Capture performance of wood-derived biochar at 35ml/min, 50 ml/min, 65 ml/min, 80 ml/min under a constant temperature of 20°C: (a) outlet CO_2 Concentration over time, (b) percentage CO_2 adsorbed, and (c) adsorption capacity in mmol/g.

At the lowest flow rate of 35 ml/min, the system achieved a high CO_2 removal efficiency of 67.43%, with an adsorption capacity of 0.0118 mmol/g (0.519mg/g). As the flow rate increased, the percentage of CO_2 adsorbed declined significantly, dropping to 30.213% at 80 ml/min, due to shorter gas-solid contact time and faster CO_2 breakthrough. Despite this reduction in efficiency, the adsorption capacity increased to 0.0178 mmol/sec (0.789 mg/g) at 80 ml/min, likely because of the higher total CO_2 delivered to the column over time. These results demonstrate that lower flow rates promote higher CO_2 removal efficiency, whereas higher flow rates enhance throughput and increase total CO_2 uptake.

This behaviour is consistent with prior studies. For instance, Shafawi et al. [44] examined the effect of varying flow rates (30-60 mL/min) on the CO_2 adsorption performance of PB700 and UAMB biochar under fixed conditions (10% CO_2, 30°C). Their

findings revealed that increasing the flow rate reduced both breakthrough time and adsorption capacity. In contrast, the lowest flow rate (30 ml/min) resulted in the longest breakthrough time and the highest CO_2 uptake. These observations reinforce the conclusion that the lowest flow rates enhance CO_2 adsorption performance by allowing sufficient time for gas diffusion and pore penetration. In a related study, Zhang et al. [13] demonstrated that KOH-activated wood biochar captured approximately 0.052 mmol/g of CO_2 from ambient air (0.04-0.15% CO_2) under fixed-bed conditions. Although the inlet CO_2 concentration was very low, the study emphasized that adequate residence time was critical for enabling CO_2 adsorption. These findings suggest that biochar is capable of capturing a measurable amount of CO_2 even under low-concentration conditions, as long as sufficient residence time is maintained. Therefore, controlling flow rate remains a key factor in achieving efficient CO_2 adsorption using biochar.

3.5 Effect of Inlet Air Temperature on CO_2 Adsorption Performance

To evaluate the effect of temperature on adsorption behavior, experiments were conducted at a constant flow rate of 35 mL/min while varying the column temperature from 5°C to 20°C. Figure 3.4 illustrate the significant enhancement in CO_2 capture performance at lower temperatures.

At 5°C, the adsorption capacity reached a maximum of 0.0140 mmol/g (0.62mg/g), with a removal efficiency of 91.815%. In contrast, at ambient conditions (20°C), the adsorption capacity and percentage adsorbed dropped to 0.519mg/g and 67.425%, respectively. The outlet CO_2 concentration curves rose more slowly at lower temperatures, indicating prolonged retention and delayed breakthrough. Additionally, the adsorption rate remained relatively high and stable over time at 5°C compared to ambient temperature, where it declined more rapidly.

From the above results, it is evident that temperature has a strong influence on CO_2 capture performance by biochar. Like many physical adsorbents, biochar exhibits an exothermic physisorption mechanism for CO_2 capture. As temperature decreases, the increase in molecular diffusion and surface adsorption energy reduces the stability of the adsorbed gas. Hence, CO_2 adsorption capacity decreases, and desorption starts

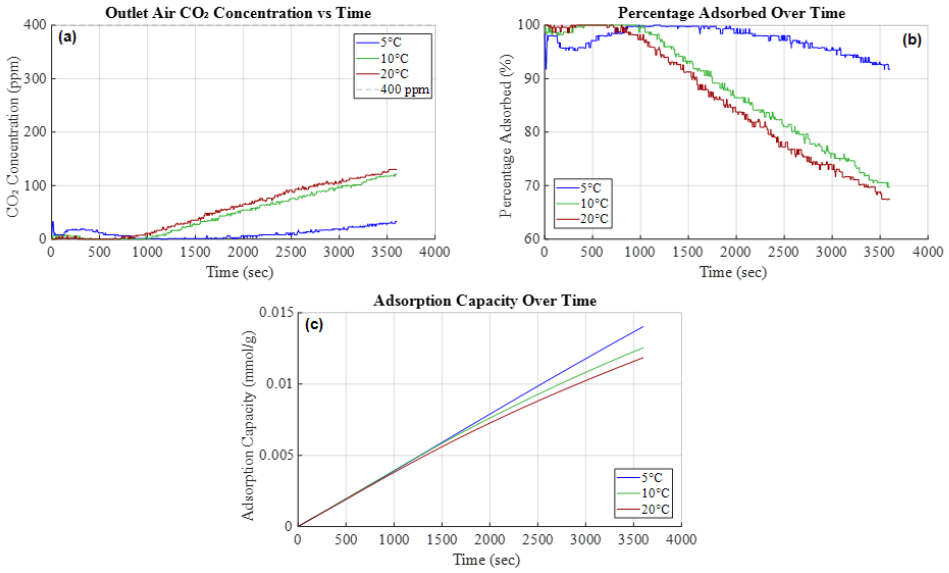

Figure 3.4: CO_2 capture performance of wood-derived biochar at 5 °C, 10 °C, and 20 °C under a constant flow rate of 35 mL/min. Subfigures: (a) outlet CO_2 concentration over time, (b) percentage of CO_2 adsorbed, and (c) adsorption capacity in mmol/g.

at higher temperatures [19]. Multiple studies have reported a negative temperature dependence for CO_2 capacity [17]. Higher temperatures lead to more activated molecules and increased frequency of collisions, thereby accelerating the reaction rate. According to reaction thermodynamics, higher temperatures also cause the reaction equilibrium to shift in the reverse direction [45]. Therefore, the effect of temperature is a combined outcome, resulting in a lower adsorption capacity at higher temperatures. Lower temperatures less than 50°C favor higher uptake [17]. For example, Gonzalez investigated the adsorption isotherms of CO_2 at 0°C, 25°C, and 50°C for activated carbon char derived from olive stone and almond shell [46]. Their results demonstrated a clear influence of temperature on CO_2 uptake capacity. CO_2 uptake on biomass-derived carbon adsorbents was reported to be approximately 2.3-3.1 mmol/g at 25°C, but significantly decreased to 0.7-0.9 mmol/g at 100°C. This indicates that low-temperature conditions (0-25°C) are highly favourable for maximizing CO_2 capture. While CO_2 uptake is highest at 0°C, operating adsorption systems at such low temperatures is not considered practical for large-scale capture processes. In DAC systems, cooling

ambient air to 0°C would also necessitate significant refrigeration input, making the process energetically and economically inefficient. Nevertheless, in this study, adsorption conducted at 5°C demonstrated notably higher CO_2 uptake compared to higher temperatures, confirming the thermodynamic advantage of low-temperature operation. This highlights the trade-off between performance and practicality in DAC system design. Another study revealed that straw-based activated carbon chars exhibited higher adsorption capacities at 25°C, approximately twice the value at 50°C [47]. Generally, increasing the adsorption temperature decreases the equilibrium capacity and lowers the apparent CO_2/N_2 selectivity [47]. Cao observed that raising the temperature from 0°C to 65°C resulted in a substantial reduction in CO_2 uptake by the biochar, ranging from 71.27% to 79.75%. This confirms the strong exothermic nature of the adsorption process [39]. This is consistent with physisorption behaviour, as higher thermal energy facilitates the release of adsorbed CO_2. At higher temperatures, surface chemistry dominates adsorption rather than micropore structure. Extremely high temperatures typically hinder capture efficiency: an increase from 30 °C to 60 °C notably decreases both breakthrough time and capacity for biomass-derived carbons [47].

3.6 Adsorption Cyclic Test

The biochar sorbent's cyclic adsorption behaviour was evaluated over nine consecutive CO_2 adsorption cycles, as illustrated in Graph 3. The adsorption capacity remained relatively stable across all cycles, with values ranging from approximately 0.014 to 0.016 mmol/g, indicating that the sorbent retained a significant portion of its uptake capability during reuse. The biochar demonstrated excellent cyclic stability and consistent adsorption capacity, which suggests it can be reused effectively in multiple CO_2 capture cycles with minimal performance loss.

This level of stability aligns with previously reported literature on biomass-derived carbonaceous adsorbents. For instance, Manya investigated the cyclic adsorption performance of physically activated biochar under dynamic conditions and reported minimal performance degradation over five consecutive CO_2 capture cycles at both 25°C and 50°C [47]. Under dry conditions at 50°C, the biochar exhibited CO_2 uptakes ranging from 0.543 to 0.571 mmol/g, with regeneration efficiencies in some cases exceeding 100%. This result, attributed by the authors to minor fluctuations in inlet CO_2

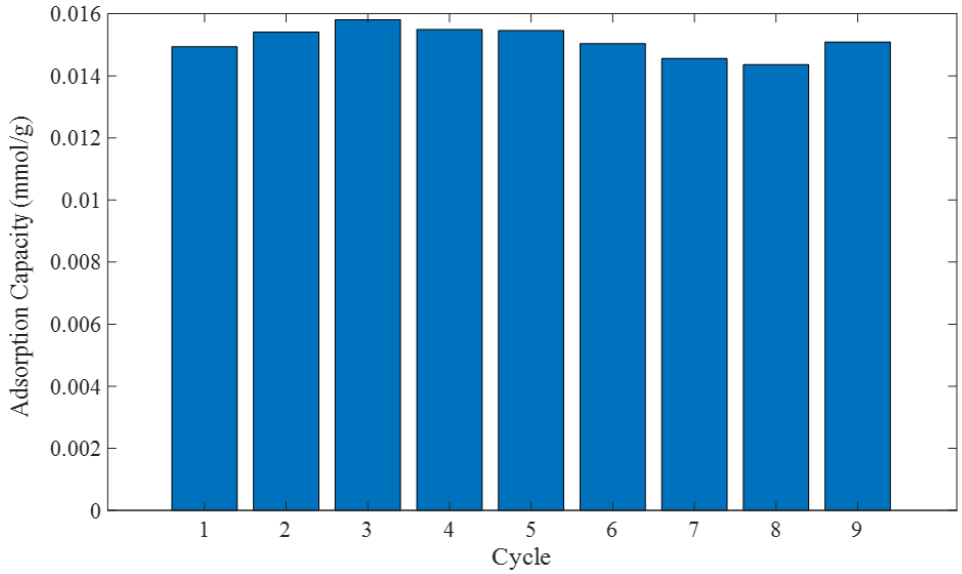

Figure 3.5: Cyclic CO_2 adsorption performance of wood-derived biochar over nine consecutive adsorption–desorption cycles. The figure demonstrates the material's stability and reusability, with consistent adsorption capacities maintained across cycles, indicating potential for long-term application in direct air capture systems.

concentrations (15.2–15.9 kPa), highlights the potential of biochar for CO_2 sequestration. These findings reinforce the excellent cyclic stability and structural robustness of biochar-based sorbents under repeated adsorption-desorption conditions, which is critical for practical CO_2 capture systems. Notably, their work also extended to humid conditions, where the biochar was tested at 50°C under 100% relative humidity. Despite the presence of moisture, the sorbent material maintained a CO_2 uptake between 0.435 and 0.542 mmol/g across ten consecutive cycles, demonstrating good retention and resilience in the presence of water vapor. Although some variability was observed in the early cycles, the capacity stabilized in later cycles, indicating that water adsorption did not irreversibly hinder CO_2 uptake. This suggests that biochar-based materials can remain effective even in moisture-rich environments, which is especially relevant for DAC applications where ambient humidity is often unavoidable. The excellent durability observed is also consistent with the findings of Huang, who tested microwave-pyrolyzed biochar over twenty adsorption–desorption cycles [49]. Their results showed only a

2–10% reduction in CO_2 capacity and minimal structural loss, particularly for high-temperature leucaena wood biochar. Similarly, the wood-derived biochar in this study showed that the biochar sorbent retained over 90% of its initial CO_2 uptake across nine cycles, affirming its reusability and regeneration potential under DAC-relevant conditions. These results support the broader conclusion that biochar is a durable, low-cost, and sustainable sorbent for removing atmospheric CO_2.

3.7 Adsorption Kinetics

3.7.1 Adsorption kinetics for lower flow rate and ambient temperature

The adsorption kinetics under a flow rate of 35 ml/min and ambient temperature (20 °C) conditions were analysed using the Pseudo-First Order (PFO) and Pseudo-Second Order (PSO) models. The fitted parameters and corresponding R-squared values are shown in the figure and summarized in the table 3.3:

Table 3.3: Kinetic parameters obtained from fitting the adsorption data to the pseudo-first-order (PFO) and pseudo-second-order (PSO) models under a flow rate of 35 mL/min and ambient temperature conditions (20 °C). The table summarizes the estimated adsorption capacities, rate constants, and corresponding coefficients of determination (R^2) for both models.

Parameter	**PFO Model**	**PSO Model**	**Unit**
Adsorption Capacity, q_e	1.990	2.610	mg/g
PFO Rate constant, k_1	2.293×10^{-4}	–	1/sec
PSO Rate constant, k_2	–	8.129×10^{-5}	1/sec
R^2	0.9924	0.9979	–

3.7.2 Adsorption kinetics for lower flow rate and lower temperature

Under a flow rate of 35 ml/min and lower temperature (5 °C) conditions, the adsorption behavior was similarly modeled using both PFO and PSO models. The obtained parameters and R-square values are shown in table 3.4:

The PSO model predicted relatively higher adsorption capacities (qe), 2.61 mg/g at ambient temperature and 3.50 mg/g at 5°C. In contrast, the PSO model estimated 1.99 and 2.53 mg/g, respectively. However, both models confirmed that CO_2 uptake is

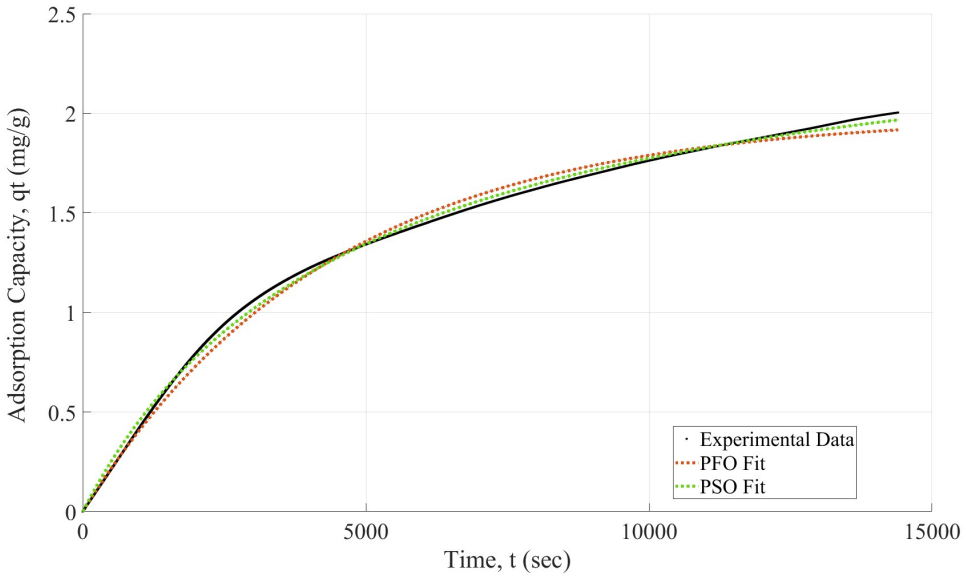

Figure 3.6: Fitting of pseudo-first-order (PFO) and pseudo-second-order (PSO) kinetic models to CO_2 adsorption data at low inlet flow rate (35 mL/min) and Ambient temperature (20 °C). Both models closely match the experimental data, indicating the presence of dual adsorption mechanisms.

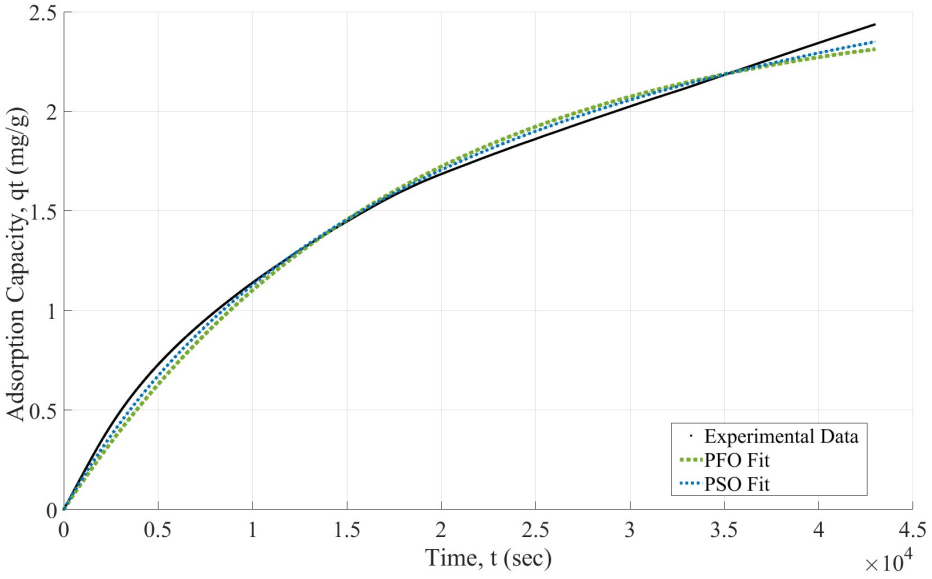

Figure 3.7: Fitting of pseudo-first-order (PFO) and pseudo-second-order (PSO) kinetic models to CO_2 adsorption data at low inlet flow rate (35 mL/min) and low temperature (5 °C). Both models closely match the experimental data, indicating the presence of dual adsorption mechanisms.

Table 3.4: Kinetic parameters obtained from fitting the adsorption data to the pseudo-first-order (PFO) and pseudo-second-order (PSO) models under low flow rate (35 mL/min) and low temperature (5 °C) conditions. The table presents the estimated adsorption capacities, rate constants, and corresponding correlation coefficients (R^2) for both models.

Parameter	**PFO Model**	**PSO Model**	**Unit**
Adsorption Capacity, q_e	2.528	3.499	mg/g
PFO Rate constant, k_1	5.715×10^{-5}	–	1/sec
PSO Rate constant, k_2	–	1.358×10^{-5}	1/sec
R^2	0.9917	0.9969	–

higher at lower temperatures. The adsorption kinetics also reduced noticeably at lower temperatures. The PFO rate constant k1 decreased from 2.293 × 10-4 sec-1 to 5.715 × 10-5 sec-1 when temperatures went down from ambient to 5°C. Similarly, the PSO rate constant k2 also fell from 8.129 × 10-5 g/mg·sec to 1.358 × 10-5 g/mg.sec. Singh and Kumar also found that the rate constant decreases with the decrease in temperature and vice versa [22].

PSO and PFO models exhibit very high R2 values under 5°C and ambient temperature. However, the PSO model provided slightly higher R2 values (0.9979 at ambient temperature and 0.9969 at 5°C) than the PFO model (0.9924 and 0.9917, respectively). When the PSO model predicted the adsorption capacity more closely with actual experimental data, the PFO model slightly underestimated qt value. Zhang also discovered that the adsorption of CO2 using bamboo biochar follows the PSO adsorption model rather than the PFO model [13]. This suggests that the adsorption process is more accurately described by a mechanism involving stronger surface attachment or a chemisorption-like interaction [50]. However, the high R2 values for both models indicate the coexistence of physisorption and chemisorption mechanisms. This dual adsorption behavior is also consistent with the surface characterization results, supporting the presence of both physical and chemical interactions on the biochar surface.

Chapter 4

Conclusion

Thermogravimetric analysis confirmed that wood-derived biochar exhibits inherent selectivity for CO_2 over N_2 and O_2, with measurable uptake only when CO_2 concentration exceeds atmospheric levels. While its high surface area and alkaline pH promote CO_2 affinity, the limited adsorption at 300 ppm CO_2 highlights that surface basicity alone is insufficient for DAC. To enhance CO_2 selectivity under DAC conditions, a combination of ultra-micropore tuning and surface functionalization of the biochar is crucial. The study demonstrated that adsorption efficiency is strongly governed by both temperature and flow rate. Peak performance was observed at 5°C and 35 mL/min, underscoring the role of thermal energy in enhancing CO_2 affinity on biochar surfaces. However, operating at lower temperatures can be energy-intensive, suggesting a practical trade-off between removal efficiency and operational cost. For large-scale DAC applications, optimizing this balance is crucial to achieving both high sorption performance and economic viability. The adsorption kinetics were best represented by the PSO model across all conditions, indicating that surface interactions primarily drive the uptake behavior. The simultaneous fit with PFO models also suggests multiple sorption pathways, consistent with findings from isotherm analyses. In summary, the material displays excellent durability, consistent regeneration, and significant potential for future improvements through surface functionalization.

Chapter 5

Recommendation

Based on the promising results of wood-derived biochar under various conditions, the following recommendations focus on improving its effectiveness for direct air capture (DAC):

- **Elemental Analysis**
  Elemental characterization is crucial for understanding the chemical composition of biochar, particularly its surface functional groups and alkaline metal contents. This clarifies the role of specific elements in CO_2 adsorption affinity and selectivity.

- **Biochar Activation to Enhance Selectivity**
  The original biochar showed moderate CO_2 selectivity. Exploring activation methods, such as chemical or physical activation, can enhance surface area, pore accessibility, and surface chemistry. These treatments enhance binding affinity and reduce competition from N_2 and O_2, thereby improving the material's suitability for low-concentration CO_2 capture.

- **Study Under Humid Conditions**
  Moisture is critical in DAC conditions. Future experiments should evaluate adsorption performance under controlled humidity to assess the influence of moisture on CO_2 capture, breakthrough time, and material stability. Understanding the competition between H_2O and CO_2 is key to DAC applications.

- **Optimizing Test Conditions**
  The study showed a trade-off between adsorption efficiency and energy cost at

low temperatures. Systematic optimization of flow rate, temperature, and column configuration is necessary to maximize adsorption while minimizing energy input and operational costs, ensuring the economic viability of DAC operation.

- **Exploring Alternative Biochars**
  To broaden the applicability of biomass-derived adsorbents, it is crucial to explore biochars produced from various feedstocks, under differing pyrolysis conditions, and with diverse structures. Comparative studies will help pinpoint the optimal candidates for scalable DAC solutions.

References

[1] H. Rashid and A. Rafey, "Solid Adsorbents for Carbon Dioxide Capture: A Review," *Chemistry and Ecology*, vol. 39, no. 7, pp. 775–791, Aug. 2023. https://doi.org/10.1080/02757540.2023.2227622

[2] A. Sodiq, Y. Abdullatif, B. Aissa, A. Ostovar, N. Nassar, M. El-Naas, and A. Amhamed, "A Review on Progress Made in Direct Air Capture of CO_2," *Environmental Technology & Innovation*, vol. 29, p. 102991, Feb. 2023. https://doi.org/10.1016/j.eti.2022.102991

[3] L. Jiang, W. Liu, R. Q. Wang, A. Gonzalez-Diaz, M. F. Rojas-Michaga, S. Michailos, M. Pourkashanian, X. J. Zhang, and C. Font-Palma, "Sorption Direct Air Capture with CO_2 Utilization," *Progress in Energy and Combustion Science*, vol. 95, p. 101069, Mar. 2023. https://doi.org/10.1016/j.pecs.2022.101069

[4] H. Azarabadi and K. S. Lackner, "A Sorbent-Focused Techno-Economic Analysis of Direct Air Capture," *Applied Energy*, vol. 250, pp. 959–975, Sep. 2019. https://doi.org/10.1016/j.apenergy.2019.04.012

[5] D. Y. Kim, W. B. Bae, H. Min, K.-H. Ryu, S. Kweon, L. M. Tran, Y. J. Kim, M. B. Park, and S. B. Kang, "Sodium Cation Exchanged Zeolites for Direct Air Capture of CO_2," *Applied Surface Science Advances*, vol. 25, p. 100664, Jan. 2025. https://doi.org/10.1016/j.apsadv.2024.100664

[6] C. Zhang, S. Sun, S. Xu, and C. Wu, "CO_2 Capture over Steam and KOH Activated Biochar: Effect of Relative Humidity," *Biomass and Bioenergy*, vol. 166, p. 106608, Nov. 2022. https://doi.org/10.1016/j.biombioe.2022.106608

[7] V. Nikulshina, M. E. Gálvez, and A. Steinfeld, "Kinetic Analysis of the Carbonation Reactions for the Capture of CO_2 from Air via the $Ca(OH)_2$–$CaCO_3$–CaO

Solar Thermochemical Cycle," *Chemical Engineering Journal*, vol. 129, no. 1, pp. 75–83, May 2007. https://doi.org/10.1016/j.cej.2006.11.003

[8] V. Nikulshina, N. Ayesa, M. E. Gálvez, and A. Steinfeld, "Feasibility of Na-Based Thermochemical Cycles for the Capture of CO_2 from Air—Thermodynamic and Thermogravimetric Analyses," *Chemical Engineering Journal*, vol. 140, no. 1, pp. 62–70, Jul. 2008. https://doi.org/10.1016/j.cej.2007.09.007

[9] C.-H. Yu, C.-H. Huang, and C.-S. Tan, "A Review of CO_2 Capture by Absorption and Adsorption," *Aerosol and Air Quality Research*, vol. 12, no. 5, pp. 745–769, 2012. https://doi.org/10.4209/aaqr.2012.05.0132

[10] A. E. Creamer, B. Gao, and M. Zhang, "Carbon Dioxide Capture Using Biochar Produced from Sugarcane Bagasse and Hickory Wood," *Chemical Engineering Journal*, vol. 249, pp. 174–179, Aug. 2014. https://doi.org/10.1016/j.cej.2014.03.105

[11] G. D. Pirngruber, F. Guillou, A. Gomez, and M. Clausse, "A Theoretical Analysis of the Energy Consumption of Post-Combustion CO_2 Capture Processes by Temperature Swing Adsorption Using Solid Sorbents," *International Journal of Greenhouse Gas Control*, vol. 14, pp. 74–83, May 2013. https://doi.org/10.1016/j.ijggc.2013.01.010

[12] P. Oleszczuk, S. E. Hale, J. Lehmann, and G. Cornelissen, "Activated Carbon and Biochar Amendments Decrease Pore-Water Concentrations of Polycyclic Aromatic Hydrocarbons (PAHs) in Sewage Sludge," *Bioresource Technology*, vol. 111, pp. 84–91, May 2012. https://doi.org/10.1016/j.biortech.2012.02.030

[13] C. Zhang, S. Sun, S. He, and C. Wu, "Direct Air Capture of CO_2 by KOH-Activated Bamboo Biochar," *Journal of the Energy Institute*, vol. 105, pp. 399–405, Dec. 2022. https://doi.org/10.1016/j.joei.2022.10.017

[14] G. Durán-Jiménez, E. T. Kostas, L. A. Stevens, W. Meredith, M. Erans, V. Hernández-Montoya, A. Buttress, C. N. Uguna, and E. Binner, "Green and Simple Approach for Low-Cost Bioproducts Preparation and CO_2 Capture," *Chemosphere*, vol. 279, p. 130512, Sep. 2021. https://doi.org/10.1016/j.chemosphere.2021.130512

[15] Y. Ji, C. Zhang, X. J. Zhang, P. F. Xie, C. Wu, and L. Jiang, "A High Adsorption Capacity Bamboo Biochar for CO_2 Capture for Low Temperature Heat Utilization," *Separation and Purification Technology*, vol. 293, p. 121131, Jul. 2022. https://doi.org/10.1016/j.seppur.2022.121131

[16] R. B. Fidel, D. A. Laird, M. L. Thompson, and M. Lawrinenko, "Characterization and Quantification of Biochar Alkalinity," *Chemosphere*, vol. 167, pp. 367–373, Jan. 2017. https://doi.org/10.1016/j.chemosphere.2016.09.151

[17] C. Goel, S. Mohan, and P. Dinesha, "CO_2 Capture by Adsorption on Biomass-Derived Activated Char: A Review," *Science of The Total Environment*, vol. 798, p. 149296, Dec. 2021. https://doi.org/10.1016/j.scitotenv.2021.149296

[18] H. Liu, H. Lin, S. Dai, and D.-e. Jiang, "Minimal Kinetic Model of Direct Air Capture of CO_2 by Supported Amine Sorbents in Dry and Humid Conditions," *Industrial & Engineering Chemistry Research*, vol. 63, no. 13, pp. 5871–5879, Apr. 2024. https://doi.org/10.1021/acs.iecr.3c04535

[19] N. A. Rashidi, S. Yusup, and B. H. Hameed, "Kinetic Studies on Carbon Dioxide Capture Using Lignocellulosic Based Activated Carbon," *Energy*, vol. 61, pp. 440–446, Nov. 2013. https://doi.org/10.1016/j.energy.2013.08.050

[20] A. Borhan, S. Yusup, J. W. Lim, and P. L. Show, "Characterization and Modelling Studies of Activated Carbon Produced from Rubber-Seed Shell Using KOH for CO_2 Adsorption," *Processes*, vol. 7, no. 11, p. 855, Nov. 2019. https://doi.org/10.3390/pr7110855

[21] Y. S. Ho and G. McKay, "Sorption of Dye from Aqueous Solution by Peat," *Chemical Engineering Journal*, vol. 70, no. 2, pp. 115–124, Jun. 1998. https://doi.org/10.1016/S0923-0467(98)00076-1

[22] V. K. Singh and E. A. Kumar, "Comparative Studies on CO_2 Adsorption Kinetics by Solid Adsorbents," *Energy Procedia*, vol. 90, pp. 316–325, Dec. 2016. https://doi.org/10.1016/j.egypro.2016.11.199

[23] S. Sadaf and H. N. Bhatti, "Evaluation of Peanut Husk as a Novel, Low Cost Biosorbent for the Removal of Indosol Orange RSN Dye from Aqueous Solutions: Batch and Fixed Bed Studies," *Clean Technologies and Environmental Policy*, vol. 16, no. 3, pp. 527–544, Mar. 2014. https://doi.org/10.1007/s10098-013-0653-z

[24] X. Xu, Y. Kan, L. Zhao, and X. Cao, "Chemical Transformation of CO_2 during Its Capture by Waste Biomass Derived Biochars," *Environmental Pollution*, vol. 213, pp. 533–540, Jun. 2016. https://doi.org/10.1016/j.envpol.2016.03.013

[25] S. Guo, Y. Li, Y. Wang, L. Wang, Y. Sun, and L. Liu, "Recent Advances in Biochar-Based Adsorbents for CO_2 Capture," *Carbon Capture Science & Technology*, vol. 4, p. 100059, Sep. 2022. https://doi.org/10.1016/j.ccst.2022.100059

[26] X. Zhang, S. Zhang, H. Yang, Y. Feng, Y. Chen, X. Wang, and H. Chen, "Nitrogen Enriched Biochar Modified by High Temperature CO_2–Ammonia Treatment: Characterization and Adsorption of CO_2," *Chemical Engineering Journal*, vol. 257, pp. 20–27, Dec. 2014. https://doi.org/10.1016/j.cej.2014.07.024

[27] J. Su, H. (H.) Teng, X. Wan, J. Zhang, and C.-Q. Liu, "Direct Air Capture of CO_2 through Carbonate Alkalinity Generated by Phytoplankton Nitrate Assimilation," *International Journal of Environmental Research and Public Health*, vol. 20, no. 1, p. 550, Jan. 2023. https://doi.org/10.3390/ijerph20010550

[28] L. Wang, M. N. P. Olsen, C. Moni, A. Dieguez-Alonso, J. M. de la Rosa, M. Stenrød, X. Liu, and L. Mao, "Comparison of Properties of Biochar Produced from Different Types of Lignocellulosic Biomass by Slow Pyrolysis at 600 °C," *Applications in Energy and Combustion Science*, vol. 12, p. 100090, Dec. 2022. https://doi.org/10.1016/j.jaecs.2022.100090

[29] A. Mukherjee, V. B. Borugadda, J. J. Dynes, C. Niu, and A. K. Dalai, "Carbon Dioxide Capture from Flue Gas in Biochar Produced from Spent Coffee Grounds: Effect of Surface Chemistry and Porous Structure," *Journal of Environmental Chemical Engineering*, vol. 9, no. 5, p. 106049, Oct. 2021. https://doi.org/10.1016/j.jece.2021.106049

[30] S. Chang, L. Wang, and L. Yao, "Properties of Sunflower Straw Biochar Activated Using Potassium Hydroxide," *Molecules*, vol. 30, no. 6, p. 1332, Jan. 2025. https://doi.org/10.3390/molecules30061332

[31] T. Song, J.-m. Liao, J. Xiao, and L.-h. Shen, "Effect of Micropore and Mesopore Structure on CO_2 Adsorption by Activated Carbons from Biomass," *New Carbon Materials*, vol. 30, no. 2, pp. 156–166, Apr. 2015. https://doi.org/10.1016/S1872-5805(15)60181-0

[32] V. Gómez-Serrano, C. M. González-García, and M. L. González-Martín, "Nitrogen Adsorption Isotherms on Carbonaceous Materials. Comparison of BET and Langmuir Surface Areas," *Powder Technology*, vol. 116, no. 1, pp. 103–108, May 2001. https://doi.org/10.1016/S0032-5910(00)00367-3

[33] Q. Chen, Y. Tian, P. Li, C. Yan, Y. Pang, L. Zheng, H. Deng, W. Zhou, and X. Meng, "Study on Shale Adsorption Equation Based on Monolayer Adsorption, Multilayer Adsorption, and Capillary Condensation," *Journal of Chemistry*, vol. 2017, p. 1496463, 2017. https://doi.org/10.1155/2017/1496463

[34] I. M. K. Ismail and P. L. Walker, "Detection of Low Temperature Carbon Gasification Using DSC and TGA," *Carbon*, vol. 27, no. 4, pp. 549–559, Jan. 1989. https://doi.org/10.1016/0008-6223(89)90005-5

[35] G. Cheng, H. Wang, B. Tan, and S. Fu, "Carbon Dioxide Prevents Oxygen Adsorption at Low-Temperature Oxidation Stage of Low-Rank Coal: Laboratory Study and Molecular Simulation," *Processes*, vol. 11, no. 8, p. 2504, Aug. 2023. https://doi.org/10.3390/pr11082504

[36] C. Zhang, Y. Ji, C. Li, Y. Zhang, S. Sun, Y. Xu, L. Jiang, and C. Wu, "The Application of Biochar for CO_2 Capture: Influence of Biochar Preparation and CO_2 Capture Reactors," *Industrial & Engineering Chemistry Research*, vol. 62, no. 42, pp. 17168–17181, Jun. 2023. https://doi.org/10.1021/acs.iecr.3c00445

[37] E. Dan, A. J. McCue, D. Dionisi, and C. F. Martín, "The Role of the Activation Heating Source on the Carbon Capture Performance of Two New Adsorbents Produced from Household-Mixed-Plastic Waste," *Journal of CO_2 Utilization*, vol. 89, p. 102950, Nov. 2024. https://doi.org/10.1016/j.jcou.2024.102950

[38] Z. Rouzitalab, D. M. Maklavany, A. Rashidi, and S. Jafarinejad, "Synthesis of N-Doped Nanoporous Carbon from Walnut Shell for Enhancing CO_2 Adsorption Capacity and Separation," *Journal of Environmental Chemical Engineering*, vol. 6, no. 5, pp. 6653–6663, 2018.

[39] A. D. Igalavithana, M. S. Ahmed, Y. J. Moon, Y. S. Ok, and J. B. Lee, "Carbon Dioxide Capture in Biochar Produced from Pine Sawdust and Paper Mill Sludge: Effect of Porous Structure and Surface Chemistry," *Science of the Total Environment*, vol. 739, p. 139845, 2020.

[40] C. Zhang, S. Sun, Y. Zhang, X. Wang, and C. Wu, "Enhancement of CO_2 Capture on Biomass-Based Carbon from Black Locust by KOH Activation and Ammonia Modification," *Energy & Fuels*, vol. 30, no. 5, pp. 4181–4190, 2016.

[41] M.-V. Nguyen and B.-K. Lee, "A Novel Removal of CO_2 Using Nitrogen-Doped Biochar Beads as a Green Adsorbent," *Process Safety and Environmental Protection*, vol. 104, pp. 490–498, 2016.

[42] J. Liu, L. Zhang, Z. Wang, X. Chen, and L. Jiang, "Direct Air Capture of CO_2 Using Biochar Prepared from Sewage Sludge: Adsorption Capacity and Kinetics," *Science of the Total Environment*, vol. 948, p. 174887, 2024.

[43] Q. Chen, Y. Tian, P. Li, C. Yan, Y. Pang, L. Zheng, H. Deng, W. Zhou, and X. Meng, "Study on Shale Adsorption Equation Based on Monolayer Adsorption, Multilayer Adsorption, and Capillary Condensation," *Journal of Chemistry*, vol. 2017, p. 1496463, 2017. https://doi.org/10.1155/2017/1496463

[44] A. N. Shafawi, N. Mohd Amer, A. R. Aghamiri, P. Lahijani, M. Mohammadi, and A. R. Mohamed, "Synthesis of Ultrasonicated Amine-Functionalized MgO-Deposited Empty Fruit Bunch (EFB)-Derived Biochar for CO_2," *[Biomass Conversion and Biorefinery 15, no. 4 (February 1, 2025): 5941–59.*, Dec. 2024. https://doi.org/10.1007/s13399-024-05465-w

[45] B. Zhao, W. Tao, M. Zhong, Y. Su, and G. Cui, "Process, Performance and Modeling of CO_2 Capture by Chemical Absorption Using High Gravity: A Review," *Renewable and Sustainable Energy Reviews*, vol. 65, pp. 44–56, Nov. 2016. https://doi.org/10.1016/j.rser.2016.06.059

[46] A. S. González, M. G. Plaza, F. Rubiera, and C. Pevida, "Sustainable Biomass-Based Carbon Adsorbents for Post-Combustion CO_2 Capture," *Chemical Engineering Journal*, vol. 230, pp. 456–465, Aug. 2013. https://doi.org/10.1016/j.cej.2013.06.118

[47] J. J. Manyà, D. García-Morcate, and B. González, "Adsorption Performance of Physically Activated Biochars for Postcombustion CO_2 Capture from Dry and Humid Flue Gas," *Applied Sciences*, vol. 10, no. 1, p. 376, 2020. https://doi.org/10.3390/app10010376

[48] L. Cao, X. Zhang, Y. Xu, W. Xiang, R. Wang, F. Ding, P. Hong, and B. Gao, "Straw and Wood Based Biochar for CO_2 Capture: Adsorption Performance and Governing Mechanisms," *Separation and Purification Technology*, vol. 287, p. 120592, Apr. 2022. https://doi.org/10.1016/j.seppur.2022.120592

[49] Y.-F. Huang, P.-T. Chiueh, and S.-L. Lo, "Carbon Capture of Biochar Produced by Microwave Co-Pyrolysis: Adsorption Capacity, Kinetics, and Benefits," *Environmental Science and Pollution Research*, vol. 30, no. 9, pp. 22211–22221, Feb. 2023. https://doi.org/10.1007/s11356-022-23734-x

[50] "An Investigation of CO_2 Adsorption Kinetics on Porous Magnesium Oxide — Request PDF," *ResearchGate*, Dec. 2024. https://doi.org/10.1016/j.cej.2015.07.055

Appendix A

Abbreviation

Table A.1: Abbreviations

Abbreviation	Meaning
AC	Activated Carbon
BDDT	Brunauer–Deming–Deming–Teller
DAC	Direct Air Capture
GISS	Goddard Institute for Space Studies
MFC	Mass Flow Controller
MOFs	Metal–Organic Frameworks
NASA	National Aeronautics and Space Administration
NDIR	Non-Dispersive Infrared (CO_2 Sensor)
NOAA	National Oceanic and Atmospheric Administration
PB700	Pristine Biochar Prepared at 700 °C
PFO	Pseudo-First Order
PSO	Pseudo-Second Order
SSA	Specific Surface Area
TGA	Thermogravimetric Analysis
UAMB	Ultrasonicated Amine-Functionalized MgO-Deposited Biochar